

Luminance-contrast properties of contour-shape processing revealed through the shape-frequency after-effect

Elena Gheorghiu^{*}, Frederick A.A. Kingdom

McGill Vision Research, Department of Ophthalmology, McGill University, 687 Pine Avenue W., Montreal, Que., Canada H3A 1A1

Received 9 January 2006; received in revised form 16 April 2006

Abstract

We investigated the first-order inputs to contour-shape mechanisms using the shape-frequency after-effect (SFAE), in which adaptation to a sinusoidally modulated contour causes a shift in the apparent shape-frequency of a test contour in a direction away from that of the adapting stimulus [Kingdom F. A. A., & Prins N. (2005a). Different mechanisms encode the shapes of contours and contour-textures. *Journal of Vision* 5(8), 463, (Abstract)]. We measured SFAEs for adapting and test contours (and edges) that differed in the contrast-polarity, scale (or blur) and magnitude of luminance contrast. The rationale was that if the SFAE was found to be reduced when adaptor and test differed along a particular dimension of luminance contrast, contour-shape mechanisms must be tuned to that dimension. Our results reveal that SFAEs manifest (i) a degree of selectivity to luminance contrast polarity for both even-symmetric (contours only) and odd-symmetric (both contours and edges) luminance profiles; (ii) a degree of selectivity to luminance scale (or blur); (iii) higher selectivity to fine compared to coarse scale for broadband edges (iv) a small preference for equal-in-contrast adaptors and tests. These results suggest that contour shapes are not encoded in the form of a sparse, cartoon-like sketch, as might be presumed by local energy (i.e. non-phase-selective) or form-cue invariant models, but instead in a form that is relatively ‘feature-rich.’

© 2006 Elsevier Ltd. All rights reserved.

Keywords: Contour-shape; Adaptation; Shape-frequency after-effect; Contrast-polarity; Blur; Contrast

1. Introduction

Psychophysical and neurophysiological studies have suggested that shape processing involves a hierarchy of mechanisms located at different levels in the visual cortex, from low (DeValois & DeValois, 1988; Koenderink & Richards, 1988; Wilson, 1991; Wilson & Richards, 1989) to intermediate (Gallant, Braun, & van Essen, 1993; Gallant, Connor, Rakshit, Lewis, & van Essen, 1996; Habak, Wilkinson, Zahker, & Wilson, 2004; Keeble & Hess, 1999; Levi & Klein, 2000; Pasupathy & Connor, 2002; Regan & Hamstra, 1992) and high levels (Gross, 1992; Ito, Fujita, Tamura, & Tanaka, 1994; Tanaka, 1996).

Much of the psychophysical evidence regarding shape processing is based on the detection and discrimination

of shapes such as sinusoidal-shaped contours (Tyler, 1973), curved contours (Kramer & Fahle, 1996; Watt & Andrews, 1982; Wilson & Richards, 1989, 1992), chevrons (Wilson, 1986), radial frequency patterns (Habak et al., 2004; Hess, Wang, & Dakin, 1999; Loffler, Wilson, & Wilkinson, 2003; Wilkinson, Wilson, & Habak, 1998) and dot-defined squares (Regan & Hamstra, 1992). Other psychophysical studies have investigated shape processing via shape after-effects (Anderson, Habak, Wilkinson, & Wilson, 2005; Anderson & Wilson, 2005; Kingdom & Prins, 2005a, 2005b; Regan & Hamstra, 1992; Suzuki, 2001, 2003; Suzuki & Cavanagh, 1998). A shape after-effect refers to the alteration in the perceived shape of a pattern following adaptation to a slightly different pattern, and is assumed to reflect changes in the activity of neurons that code for shape. Some shape after-effects are assumed to implicate global shape mechanisms because they transfer across size (Regan & Hamstra, 1992; Suzuki & Cavanagh, 1998) or are attention-dependent (Suzuki, 2001, 2003).

^{*} Corresponding author.

E-mail address: elena.gheorghiu@mail.mcgill.ca (E. Gheorghiu).

In spite of the fact that the adaptation patterns in these studies were static, various control experiments make it unlikely that the after-effects were caused either by after-images or adaptation to local orientation, as was shown some time ago to be the case for curvature adaptation using static adaptors (Blakemore & Over, 1974; Stromeyer & Riggs, 1974).

Kingdom and Prins (2005a, 2005b) demonstrated a novel after-effect termed the *shape-frequency after-effect*, or SFAE, using a non-static adaptation stimulus. They showed that adaptation to a sinusoidal-shaped contour causes a shift in the perceived shape-frequency of a test contour in a direction away from that of the adapting stimulus. The SFAE is the shape analog of the well-known spatial-frequency after-effect found with luminance gratings (Blakemore & Sutton, 1969). The SFAE occurs even though the shape-phase of the adaptation stimulus is randomized every half second during the adaptation period. The reader can experience the SFAE in Fig. 1. If one moves one's eyes back and forth along the marker between the pair of adapting contours on the left for about a minute, and then shifts gaze to the spot on the right, the two test contours, which have the same shape-frequency, should appear different in shape frequency. Thus adaptation to a contour of a given shape-frequency makes a lower-shape-frequency test contour appear lower in shape-frequency and a higher-shape-frequency test contour appear higher in shape-frequency. A movie demonstration of the SFAE can be found at <http://www.mvr.mcgill.ca/Fred/research.htm#contourShapePerception>.

What mechanisms mediate the SFAE? The SFAE occurs even though the shape-phase of the adaptation contour is randomly changed every half second during adaptation. This might be taken to imply that the effect could not be mediated by the tilt after-effect (TAE) because the orientation content of the adaptor at any one visual location is constantly changing. However, the geometrical relationships between adaptor and test are such that the TAE cannot on a priori grounds be ruled out. Recently however, in a preliminary report, Kingdom and Gheorghiu (2006) have shown that sine-wave-shaped adaptors induce equal-sized SFAEs in square-wave-shaped not just sine-wave-shaped tests. At any one visual location the set of possible orientations from a phase-randomized sine-wave adaptor will always be such as to produce equal and opposite TAEs in the oriented segments of a square-wave test, and so local TAEs would simply cancel. Hence, the TAE is unlikely to be the cause of the SFAE. Kingdom and Gheorghiu (2006) also found sizeable SFAEs from adaptor and test pairs that had the same global average curvature, thus ruling out global average curvature as the spatial feature underlying the SFAE. They also ruled out global spatial frequency and density (e.g. see Durgin, 1996, 2001; Durgin & Proffitt, 1996; Durgin & Huk, 1997) by showing that the perceived spacing/density of an array of identically oriented elements was unaffected by adaptation to the sine-wave-shaped contour. Finally, Kingdom and Gheorghiu (2006) showed that

SFAEs reached asymptotic levels when the test contour was gated down to just half a cycle of shape modulation centered on the peak or trough. This suggests that the SFAE operates locally on contour segments that have constant sign of curvature. Thus the SFAE is likely mediated by intermediate-level curvature detectors that lie beyond those responsible for local orientation and positional adaptation, but prior to those involved in global shape analysis.

The cross-sectional luminance profiles of natural contours and edges can vary in luminance phase, scale (or blur) and contrast. Models of early human vision designed to detect contours and edges invariably use operators that are sensitive to these luminance attributes; for example bandpass filters tuned to spatial frequency. However, the extent to which information about the luminance profile is preserved for higher visual functions, such as shape processing, is not at all well understood. Some models, termed here 'feature-rich' explicitly represent the luminance scale and luminance phase of contour/edge segments for higher stages of processing (Hesse & Georgeson, 2005; Marr, 1982; Marr & Hildreth, 1980; Watt, 1988; Watt & Morgan, 1985). Other models, termed here 'feature-agnostic,' do not represent luminance phase for higher stages of processing, for example those based on local contrast energy (e.g. Moronne & Burr, 1988—see Section 7 for details).

The evidence for visual mechanisms that are selective for luminance phase comes mainly from studies that have measured phase discrimination at contrast threshold for line-like, edge-like and gabor stimuli (reviewed by Huang, Kingdom, & Hess, 2006). In general, studies of luminance phase discrimination have restricted themselves to phases represented by opposite contrast-polarities of edge-like and bar-like stimuli, and from now on our discussions of luminance phase will be couched in terms of contrast polarities. With regard to shape perception, contrast-polarity consistency has been shown to be an advantage for illusory contour perception (He & Ooi, 1998), and contrast-polarity specificity has been demonstrated for the luminance spatial frequency after-effect (Blake, Overton, & Lema-Stern, 1981; Blakemore & Sutton, 1969; Burton, Nagshineh, & Ruddock, 1977; DeValois, 1977a, 1977b; Fiorentini, Baumgartner, Magnusson, Schiller, & Thomas, 1990), but not for the tilt after-effect (Magnussen & Kurtenbach, 1979). However to our knowledge no study has investigated whether contour-shape mechanisms are contrast-polarity-tuned.

With regard to luminance scale, or blur, this is by definition important for edge blur perception (Hesse & Georgeson, 2005; Watt & Morgan, 1985), and generally assumed to be an important factor for both edge detection (Marr, 1982; Marr & Hildreth, 1980; Watt & Morgan, 1985) and the reconstruction of an image from an edge representation (Elder & Sachs, 2004). For shape, Wilson and Richards (1989) have shown that curvature discrimination thresholds for contours were unimpaired by high-pass but impaired by low-pass luminance filtering. On the other hand, Hayes, Kingdom, and Prins (2002) found that the

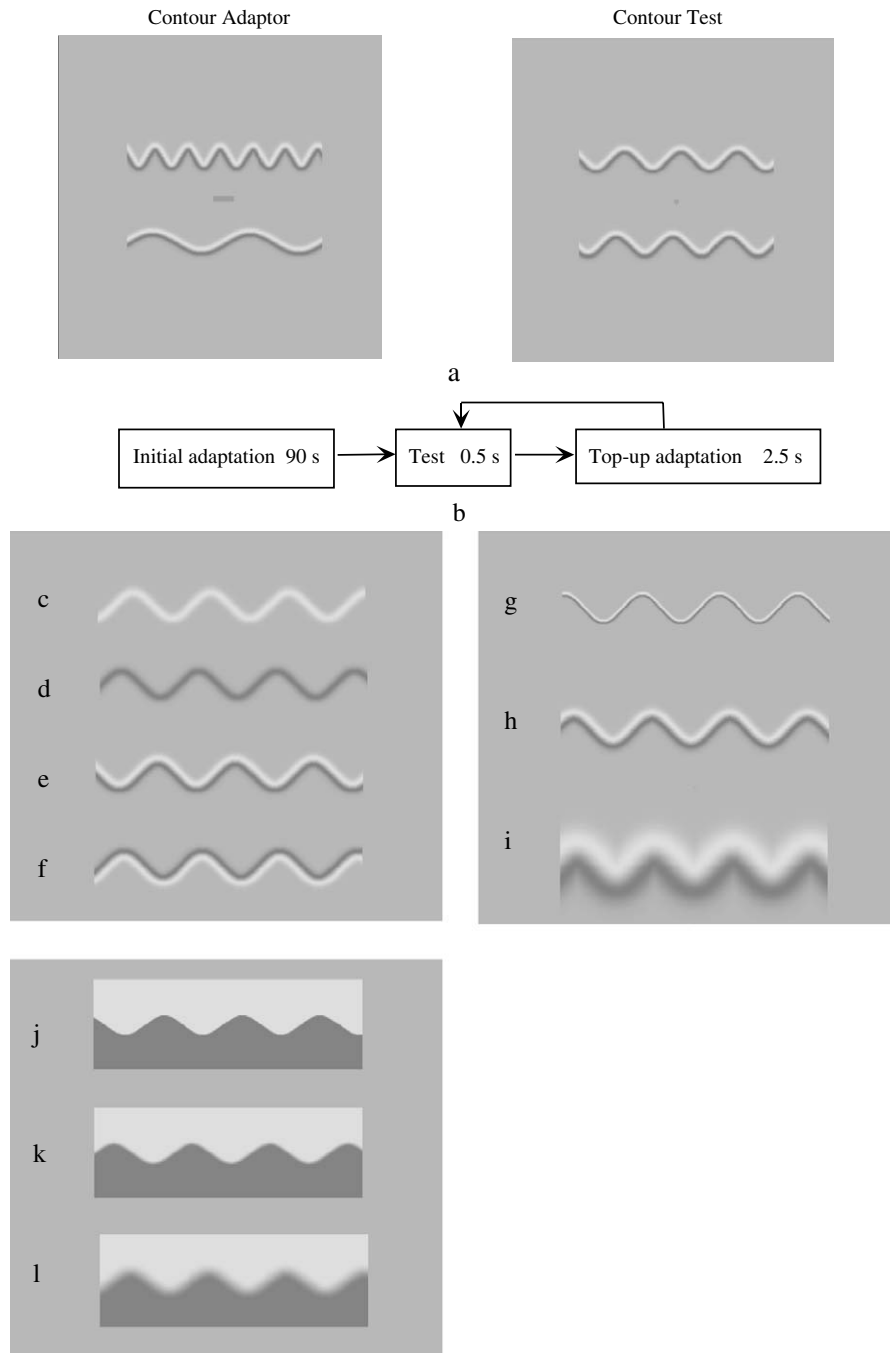


Fig. 1. Stimuli used in the experiments. In (a) one can experience the SFAE by moving one's eyes back and forth along the marker located midway between the pair of adapting contours in the left-hand panel for about 90s, and then shift one's gaze to the middle of the test contour pair in the right-hand panel. The two test contours, which have the same shape frequency, should look different in shape frequency. Thus adaptation to a contour of a given shape-frequency makes a lower-shape-frequency test contour appear lower in shape-frequency and a higher-shape-frequency test contour appear higher in shape-frequency. (b) Schematic representation of the adapting and test procedure (see also text for details). Example contours: (c) 'bright'; (d) 'dark'; (e) 'bright-dark,' and (f) 'dark-bright,' (g) 'fine scale,' (h) 'intermediate scale,' (i) 'coarse scale.' Example edges: (j) 'sharp,' (k) 'slightly blurred' and (l) 'highly blurred,' corresponding to σ_s of 0.033, 0.104 and 0.247 deg, respectively.

detection of the low shape-frequency component of a jagged, or fractal edge, was not significantly impaired by either high-pass or low-pass filtering. These two studies agree that fine luminance scales can mediate the efficient coding of contour shape but disagree as to whether coarse luminance scales also do so. In this study we use the SFAE to determine whether contour shape mechanisms are tuned

to luminance scale and whether some scales contribute more than others to contour shape processing.

With regard to luminance contrast, while it is known that contrast gain control mechanisms regulate the sensitivity of neurons to gratings, contours and edges (Greenlee & Heitger, 1988; Greenlee & Thomas, 1992, 1993; Hammett, Snowden, & Smith, 1994; Harris & Calvert, 1989; Pantle &

Sekuler, 1968; Snowden, 1994; Wilson & Humanski, 1993), to our knowledge there is no evidence that contour-shape mechanisms are tuned to contrast. Indeed, Suzuki (2001) has reported that after-effects for contour shapes induced by very brief adaptation rapidly saturate at low contrast are therefore mainly independent of contrast, a finding complemented by single unit recordings of neurons in the higher visual areas that are responsive to faces (Rolls & Baylis, 1986).

In the present study, we use the SFAE to test whether shape-encoding mechanisms are tuned to (a) contrast-polarity, (b) luminance scale, or blur, and (c) luminance contrast. To do this we have compared SFAEs for adaptor-and-test combinations with the same luminance attributes with adaptor-and-test combinations having different luminance attributes. We make the assumption that if SFAEs are significantly greater for same-attribute compared to different-attribute combinations, then contour-shape mechanisms are tuned to that attribute. The results should have wider theoretical value in that we will learn the extent to which contour-shape encoding is ‘feature-rich’ as opposed to ‘feature-agnostic.’

Before proceeding, we mention one further novel aspect of our study. Conventional methods of contour construction produce contours that vary in their width, especially for contours with high curvature. Because we were interested in the luminance scale tuning of contour shape perception, we felt it prudent to construct our contours with luminance profiles that were constant in width and whose orientations were always perpendicular to the tangent of the contour. The method used to achieve this is described in the [Appendix A](#).

2. General methods

2.1. Observer

Five subjects participated in the experiments, the two authors (EG and FK) and three naive volunteers. All subjects had normal or corrected-to-normal visual acuity.

2.2. Stimuli

The stimuli were generated by a VSG2/5 video-graphics card (Cambridge Research Systems) with 12-bits contrast resolution, and presented on a calibrated, γ -corrected Sony Trinitron monitor (120 Hz frame rate, 1024×768 spatial resolution). The mean luminance of the monitor was 42 cd/m^2 .

Adapting and test stimuli consisted of pairs of 2D sinusoidal-shaped contours or edges, as shown in [Fig. 1](#). The stimuli were presented in the center of the monitor on the mean luminance background. The two adapting contours were centered 2 deg above and below the fixation marker. Each contour filled an area 8 (width) \times 4 (height) deg. All experiments used pairs of contour or edge adaptors, with shape frequencies 0.25 and 0.75 c/deg, giving a geometric mean shape frequency of 0.43 c/deg.

The cross-sectional luminance profiles of the contours were of three types. *Even-symmetric* profiles ([Fig. 1c](#) and [d](#)) were generated according to a Gaussian function:

$$L(d) = L_{\text{mean}} \pm L_{\text{mean}} \cdot C \cdot \exp[-(d^2)/(2\sigma^2)], \quad (1)$$

where d is the distance from the centre of the contour in a direction perpendicular to the tangent, L_{mean} is mean luminance of 42 cd/m^2 , C contrast and σ the space-constant, or standard deviation, that determines the width of the contour. The \pm sign determined the polarity of the Gaussian (bright or dark). *Odd-symmetric* profiles ([Fig. 1e–i](#)) were generated according to a first derivative (1D) of a Gaussian function:

$$L(d) = L_{\text{mean}} \pm L_{\text{mean}} \cdot C \cdot \exp(0.5) \cdot d/\sigma \cdot \exp[-(d^2)/(2\sigma^2)]. \quad (2)$$

In this particular form of a 1D Gaussian, the term $\exp(0.5)$ gives the profile the same peak, or trough value as the Gaussian function in [Eq. \(2\)](#). *Edge* luminance profiles were constructed according to the same function used to generate the odd-symmetric contours, with the constraint that the profile remained asymptotic at the peak of the function. Example edge stimuli of various σ s are shown in [Fig. 1j–l](#).

Contrast C was set to 0.5 except unless otherwise stated. Since the peak, or trough values of the 1D Gaussian profiles were the same as the Gaussian profiles, this meant that the odd-symmetric contours had double the Michelson contrast of the even-symmetric contours. Equalizing the peaks/troughs rather than Michelson contrasts of the Gaussian and 1D Gaussian functions was somewhat of an arbitrary decision. However, given the weak dependence of the SFAE on absolute contrast, and the fact that we never used the Gaussian and 1D Gaussian contours together in any condition, we assume that this does not matter. The method used to construct sinusoidal shaped contours of constant width is given in the [Appendix A](#).

2.3. Procedure

A schematic representation of the adapting and test procedure is shown in [Fig. 1b](#). Each session began with an initial adaptation period of 90 s, followed by a repeated test of 0.5 s duration interspersed with top-up adaptation periods of 2.5 s. During the adaptation period, the shape phase was changed randomly every 0.5 s in order to prevent the formation of afterimages and to minimize the effects of local orientation adaptation. The presentation of the test contour was signaled by a tone. The display was viewed in a dimly lit room at a viewing distance of 100 cm. Subjects were required to fixate on the marker placed between each pair of contours/edges for the entire session. A head and chin rest helped to minimize head movements.

A staircase method was used to estimate the magnitude of the SFAE. During the test period the geometric mean shape frequency of the two test contours was always held constant at 0.43 c/deg, while the computer

varied the relative shape frequencies of the two tests in response to the subject. At the start of the test period the ratio of the two test shape frequencies was set randomly between 0.33 and 3. On each trial subjects indicated via a button press whether the upper or lower test contour had the higher perceived shape-frequency. In response the computer changed the ratio of shape frequencies by a factor of 1.06 for the first five trials and 1.015 thereafter, and in a direction opposite to that of the response, i.e. towards achieving a point of subjective equality, or PSE. The session was terminated after 25 trials. The shape-frequency ratio at the PSE was calculated as the geometric mean ratio of test shape-frequencies over the last 20 trials. Eight measurements were made for each condition, four in which the upper adaptor had the higher shape-frequency (75 c/deg) and four in which the lower adaptor had the higher shape-frequency. In addition we measured for each condition the PSE shape-frequency ratio in the absence of the adapting stimulus. To obtain an estimate of the SFAE we calculated the difference between each measurement of with-adaptor PSE log shape-frequency ratio with the mean no-adaptor PSE log shape-frequency ratio, and then calculated the mean and standard error of the differences across measurements.

3. Experiment 1: Effect of contrast-polarity

Here, we examine whether contour-shape mechanisms are selective for contrast-polarity. We used contours with even-symmetric (Fig. 1c and d) and odd-symmetric (Fig. 1e and f) luminance profiles, and edges (Fig. 1j). For the contours there were six conditions: (a) adaptor and test both ‘bright’; (b) adaptor and test both ‘dark’; (c) adaptor ‘bright’ and test ‘dark’; (d) adaptor ‘dark’ and test ‘bright’; (e) adaptor and test both ‘bright–dark,’ and (f) adaptor ‘bright–dark’ and test ‘dark–bright.’ For the even-symmetric contours we used a σ of 0.104 deg. For the odd-symmetric contours we used σ s of 0.044, 0.104 and 0.247 deg (Fig. 1g–i), corresponding to fine, intermediate and coarse scales. For the edges we used a σ of 0.033 deg.

Fig. 2a shows SFAEs for all six conditions for the intermediate scale contours ($\sigma = 0.104$ deg). Same adaptor-test contrast-polarities are shown as white bars and opposite adaptor-test contrast-polarities are shown as gray bars. The results show that SFAEs are significantly reduced when adapting and test contours are of opposite contrast-polarity. The SFAEs are broadly similar for even-symmetric and odd-symmetric contours of same contrast-polarity. Fig. 2b shows that the same result holds for odd-symmetric contours at the fine (F), intermediate (I) and coarse (C) luminance scales. The difference between same contrast-polarity and opposite contrast-polarity SFAEs appears to increase somewhat as the contour become thicker.

In order to test whether the SFAEs for the same and opposite adaptor-test conditions were significantly different we

performed a two-factor within-subjects ANOVA (analysis of variance) analysis with Phase (bright and dark even-symmetric and odd-symmetric) and Contrast-Polarity (same and opposite) as factors on the data shown in Fig. 2a. SFAEs were significantly different for the same and opposite adaptor-test combinations ($F(1,3) = 1052.69; p < 0.001$). In addition, we performed a within-subjects ANOVA analysis to test whether the opposite contrast-polarity SFAEs (gray bars in Fig. 2a) were significantly different from zero, that is, significantly different from the non-adapted condition. Opposite contrast-polarity SFAEs were not quite significantly different from zero ($F(1,3) = 6.5; p = 0.0846$).

4. Experiment 2: Effect of luminance scale for narrowband contours

In this experiment, we examined whether contour-shape mechanisms are tuned to luminance scale, or blur. Adaptor and test contours were constructed with odd-symmetric luminance profiles of various σ s. Example contours are shown in Fig. 1g–i. There were nine values of σ_{adapt} : 0.033, 0.044, 0.058, 0.078, 0.104, 0.138, 0.185, 0.247 and 0.330 deg, and three values of σ_{test} : 0.044, 0.104 and 0.247 deg, corresponding to fine, intermediate and coarse scales.

Fig. 3 shows SFAEs as a function of σ_{adapt} for intermediate (Fig. 3a), fine (Fig. 3b, light gray circles) and coarse (Fig. 3b, dark gray triangles) test stimuli. The results show that all SFAEs peak when the adapting and test contours have the same σ , but that the tuning to σ_{adapt} is broad. There is also a curious bimodal function seen in both EG’s and FK’s coarse-scale test condition, where an unexpected secondary peak in the SFAE is found for very fine-scale adapting contours. This hints at the possibility that fine-scale inputs contribute disproportionately to contour shape processing.

The odd-symmetric test contours employed in this experiment are relatively narrowband in luminance spatial frequency. The visual system can only recruit for contour shape processing those first-order inputs stimulated by the test contour. Thus, while the results of this experiment tell us that contour shape mechanisms are to a degree tuned to luminance spatial frequency, they do not tell us whether only a subset, or all luminance spatial frequencies contribute equally to contour shape processing when the test stimulus is broadband. Given the hint in our data that high spatial frequencies contribute disproportionately to the SFAE, we decided to assess the relative contributions of different luminance scales to contour shape processing in broadband stimuli.

5. Experiment 3: Effect of luminance scale for broadband edges

In order to assess the relative contributions of fine and coarse luminance scales to the SFAE in broadband-in-luminance stimuli, we employed the test edge with σ of

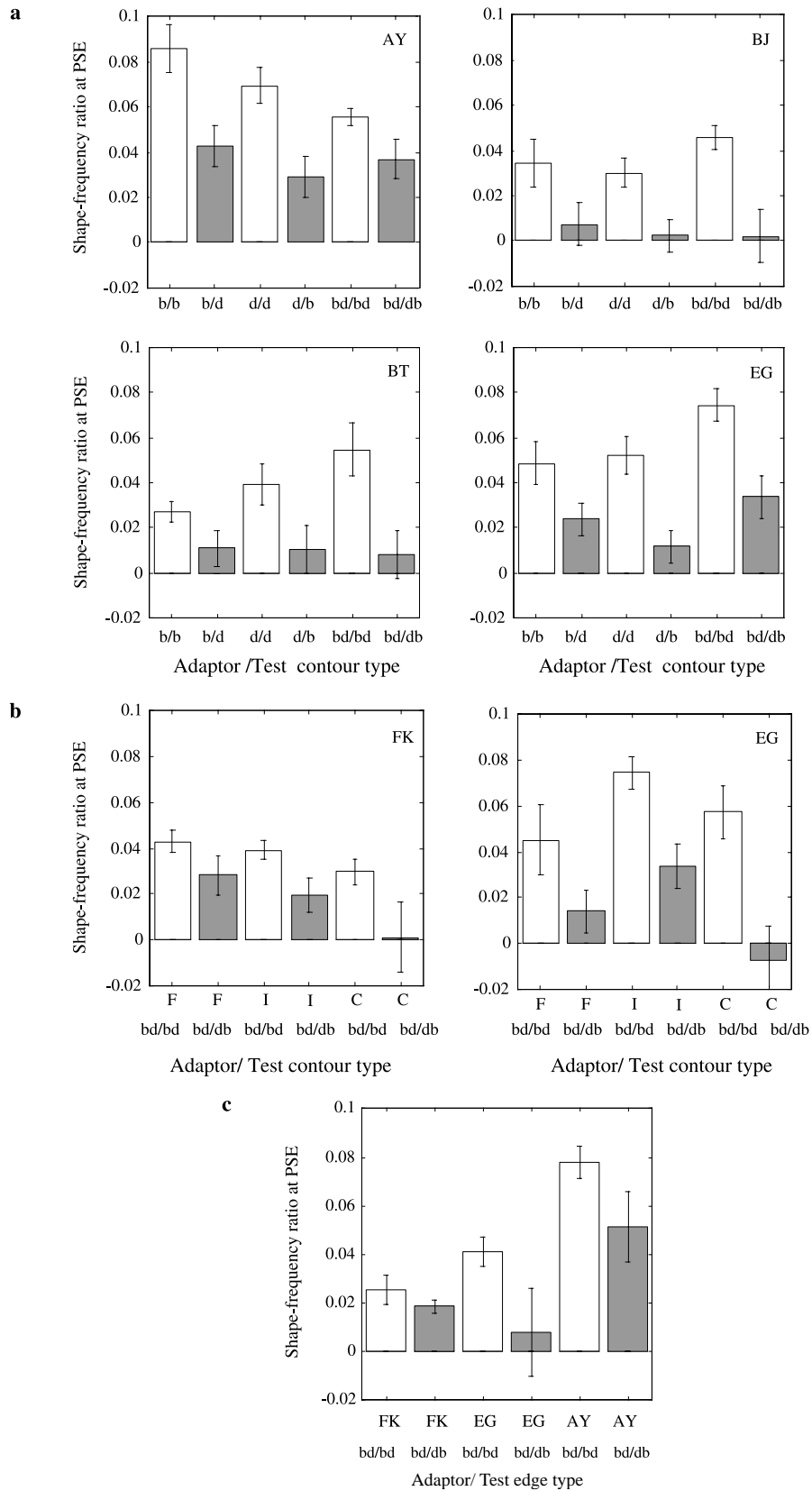


Fig. 2. (a) SFAEs for adaptor-test combinations with the same (white bars) and opposite (gray bars) contrast-polarity. Different types of contour are indicated as follows: 'b'- bright; 'd'- dark; 'bd'- bright-dark, and 'db'- dark-bright. b/d means bright adaptor and dark test etc. (b) SFAEs obtained for adaptor-test combinations with the same (white bars) and opposite (gray bars) contrast-polarity for contours of fine (F), intermediate (I), and coarse (C) luminance scales. (c) SFAEs obtained for edges with the same (white bars) and opposite (gray bars) contrast-polarity.

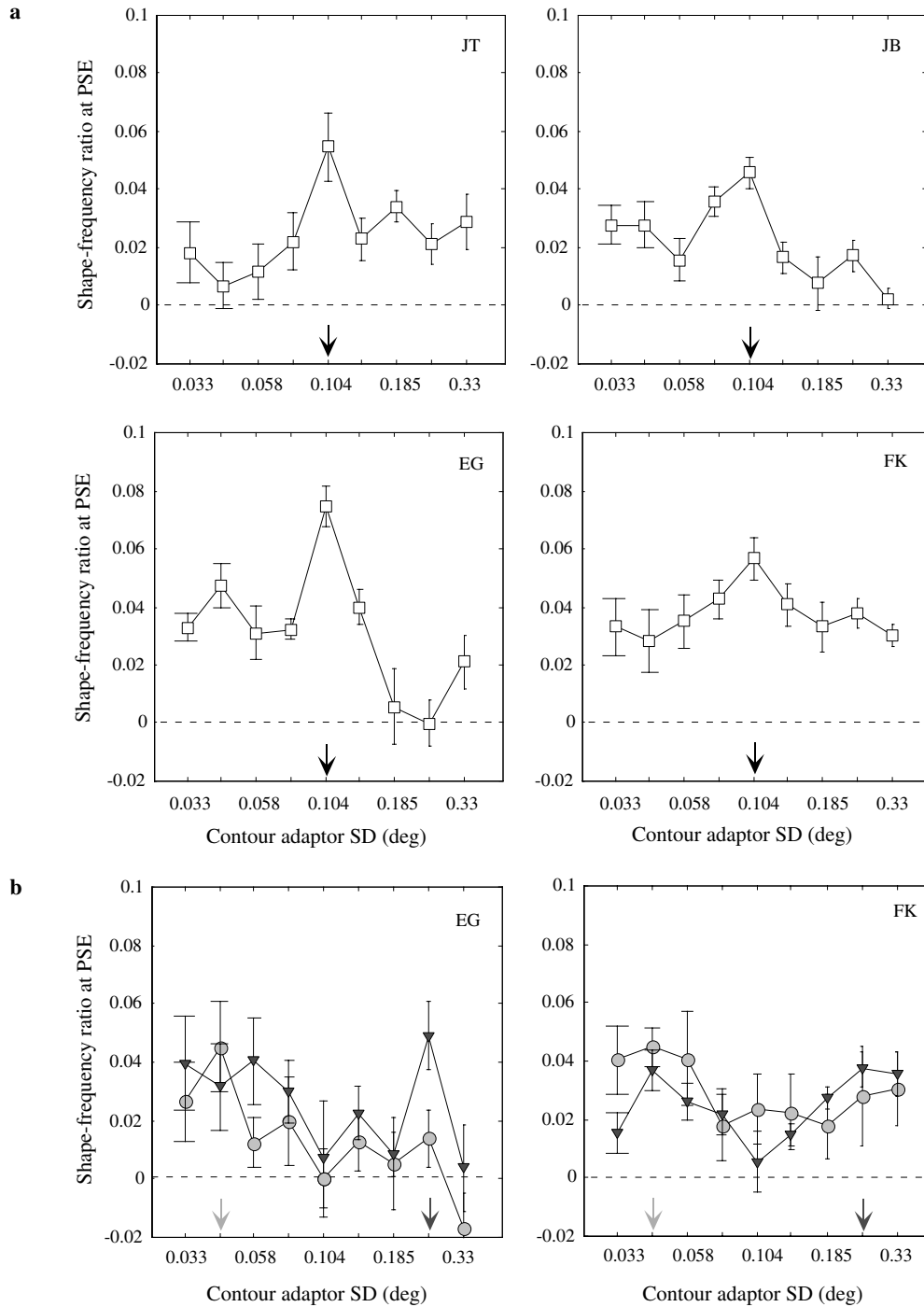


Fig. 3. SFAEs as a function of the luminance scale of the contour adaptor, σ_{adapt} . The top four plots (a) show SFAEs for intermediate scale test contours ($\sigma = 0.104$). The bottom two plots (b) show SFAEs for both fine ($\sigma = 0.044$ deg) test contours (light gray circles) and coarse ($\sigma = 0.247$ deg) test contours (dark gray triangles).

0.033 deg shown in Fig. 1j. For adaptors we used both narrowband-in-luminance odd-symmetric contours (Fig. 1g–i) and broadband-in-luminance edges (Fig. 1j–l), with the same range of σ_{adapt} as in the previous experiment. Example edge stimuli are shown in Fig. 1j–l for σ_{adapt} of 0.033, 0.104 and 0.247 deg, respectively. If the shapes of broadband test edges are processed by mechanisms that recruit

luminance inputs from across a wide range of scales, then we should expect that (a) contour adaptors of all σ will produce equal-sized SFAEs, (b) a sharp edge adaptor will produce significantly larger SFAEs than any of the contour adaptors, and (c) as the edge adaptor σ increases there will be a steady decline in the SFAE. If, on the other hand, contour-shape processing in broadband stimuli is driven

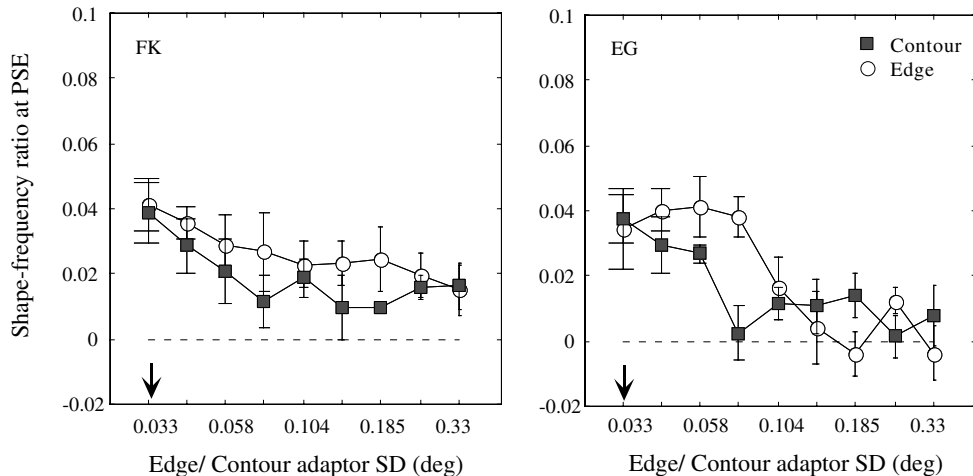


Fig. 4. SFAEs for a sharp test edge ($\sigma = 0.033$ deg) obtained from narrowband-in-luminance odd-symmetric contour adaptors (filled squares) and broadband-in-luminance edge adaptors (open circles) of various σ .

predominantly by fine-scale luminance inputs, we should expect a steep and similarly shaped decline in SFAEs with σ , for both contour and edge adaptors.

Fig. 4 shows the results. SFAEs for fine-scale contour and sharp edge adaptors are very similar (the most left-hand points), and SFAEs decline gradually with σ_{adapt} for both contour and edge adaptors. The decline is not equal however, with SFAEs for edge adaptors declining less sharply (open symbols) than for contour adaptors (filled symbols). These results suggest that with broadband stimuli, contour shape mechanisms recruit from across a range of luminance scale inputs, but give greater weighting to fine luminance scales.

6. Experiment 4: Effect of contrast

In this experiment, we investigate whether the SFAE is tuned to contrast. If the SFAE is tuned to contrast, we should expect SFAEs to be biggest when the adaptor and test contrasts are the same, irrespective of the actual contrast. We used odd-symmetric contours with a σ of 0.104 deg at three contrasts, 0.05, 0.15 and 0.45. Several adaptor-test contrast conditions were tested: (i) equal-in-contrast adaptors and tests; (ii) high contrast adaptors and low contrast tests, and (iii) low contrast adaptors and high contrast tests. Thus, given three contrasts and three adaptor-test combinations there were nine adaptor-test contrast combinations. We considered three possible outcomes: (i) SFAEs are biggest for equal-in-contrast adaptors and tests, irrespective of overall contrast; (ii) SFAEs increase with the contrast of either adaptor or test; (iii) SFAEs increase with the difference in contrast between adaptors and tests.

Fig. 5 shows results for three subjects. SFAEs are shown as a function of (a) log adapting contrast, (b) log test contrast, (c) signed log adaptor-to-test contrast ratio, and (d) absolute log adaptor-to-test contrast ratio. The first thing to notice is that SFAEs do not vary considerably with any of the functions of contrast. However, of the four ways

of plotting the results, the most noticeable trend is in Fig. 5d, which plots SFAEs against absolute log adaptor-to-test contrast ratio. For this plot the R^2 (coefficient of determination) values based on linear regression fits to the data for each subject are the highest, on average 0.49 (see insets in Fig. 5). Fig. 5c indicates that there is a slight asymmetry in this result, in that SFAEs are larger for low-contrast adaptors combined with high-contrast tests compared to high-contrast adaptors combined with low-contrast tests.

7. General discussion

In the introduction, we described the evidence that the SFAE most likely reflects the operation of intermediate-level shape-encoding mechanisms involved in encoding the shapes of contour segments with constant sign of curvature. Therefore for this level of contour-shape processing our results have revealed (i) a degree of selectivity to contrast-polarity for both even-symmetric contours and odd-symmetric contours and edges; (ii) a degree of selectivity to luminance scale; (iii) greater weighting for fine compared to coarse scales in the encoding of broadband edges; (iv) a small degree of tuning to luminance contrast.

Both the even and odd symmetric contours showed selectivity to luminance contrast polarity. One plausible physiological basis of this result is that contour shapes are represented by patterns of ON- and OFF-centre neuron responses (Schiller, 1982, 1984; Schiller, Sandell, & Maunsell, 1986; and see Huang et al., 2006). Although not significantly different from the un-adapted condition (baseline), the small sized SFAEs found for opposite contrast-polarity adaptor/test combinations may result from the incomplete isolation of ON and OFF responses by our suprathreshold-contrast stimuli. For example the bright contour in Fig. 1c would predominantly but not exclusively stimulate ON-centre filters, and the dark contour would predominantly but not exclusively stimulate OFF-centre filters.

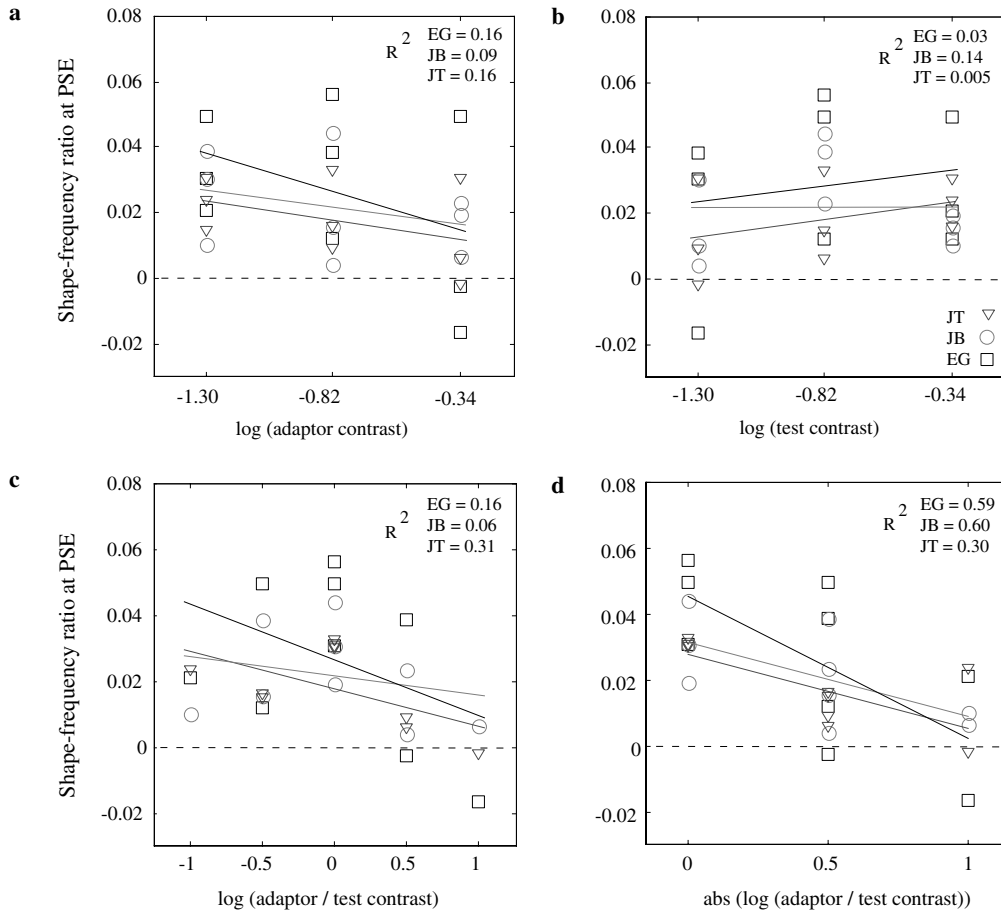


Fig. 5. Effect of contrast on the SFAE. SFAEs are shown as a function of (a) log adapting contrast, (b) log test contrast, (c) signed log adapting-to-test contrast ratio, and (d) absolute log of adapting-to-test contrast ratio. See test for details.

The results of Experiment 3 suggest that broadband edge shape mechanisms draw disproportionately from fine luminance scales. This is consistent with the results of Wilson and Richards (1989), who showed that curvature discrimination thresholds for contours were unimpaired by high-pass but impaired by low-pass luminance filtering, the impairment being especially large at high curvatures. On the other hand the results are not consistent with Hayes et al. (2002). Hayes et al., measured the detectability (i.e. not discriminability) of sinusoidal shapes. They showed firstly that the shapes of smooth contours were more-or-less equally detectable irrespective of whether they were fine or coarse, and secondly that the detectability of the low frequency shape components of jagged, or fractal edges were not significantly impaired by either high-pass or low-pass luminance filtering. The results from Hayes et al. (2002) suggest that both coarse and fine scales can mediate contour shape perception with equal efficiency. The most likely reason for the discrepancy between the present (and Wilson and Richards') results and Hayes et al. (2002) is that the last of these studies involved curvatures that were generally very low and therefore perhaps more effectively represented by coarse-scale luminance filters.

SFAEs showed a small degree of tuning to contrast in that they were largest when adaptor and test contrasts were

the same. However, it would be imprudent to conclude from this finding that separate shape-encoding mechanisms exist for different contrasts. It is possible that the contrast dependency of the SFAE results from the types of contrast-gain control mechanism known to be a feature of cortical neural function (Bonds, 1989, 1991; Heeger, 1992; Scalar, Ohzawa, & Freeman, 1982, 1985), though we are not aware of any model of contrast gain control that predicts a maximum after-effect when adaptors and tests have the same contrast. Further experiments and modeling will be needed to cast further light on this finding.

7.1. First-order properties of the SFAE in relation to other shape after-effects

Unlike the SFAE, the tilt after-effect is unselective for contrast-polarity (Hanly & MacKay, 1979; Magnussen and Kurtenbach, 1979). Like the SFAE, face after-effects (Yamashita, Hardy, De Valois, & Webster, 2005) and figural after-effects for simple two-dimensional patterns (Burton et al., 1977; DeValois, 1977a) are contrast-polarity selective. For example, Yamashita et al. (2005) showed that shifts in the perceived featural content of faces following adaptation to distorted versions of faces were strongly contrast-polarity selective. Given that the SFAE is presumably

mediated by relatively high-level shape-encoding processes, these findings taken together might suggest a trend towards greater contrast-polarity specificity with processing level. However, the fact that the luminance spatial-frequency after-effect, which like the tilt after-effect is presumably low-level, shows specificity for contrast-polarity (Blake-more & Sutton, 1969; Blake et al., 1981; Burton et al., 1977; DeValois, 1977a, 1977b; Fiorentini et al., 1990), suggests instead that the polarity-nonspecificity of the tilt after-effect may be an anomaly rather than an indication of a general trend.

As with the SFAE, the tilt after-effect exhibits luminance spatial-frequency tuning (Held, Shattuck-Hufnagel, & Moskowitz, 1982; Fiorentini et al., 1990). Yamashita et al. (2005) also showed that face after-effects were strongly selective for spatial frequency. Thus, the SFAE shares spatial-frequency selectivity with both low and high level shape after-effects.

With regard to contrast, Suzuki (2001) and Anderson et al. (2005) reported that global shape after-effects saturated at low adapting contrasts and were thus largely independent of contrast. Yamashita et al. (2005) showed that face after-effects had *weaker* selectivity for changes in contrast. We also showed that SFAEs varied little with adapting contrast, though unlike other studies, we found the biggest SFAEs when adaptor and test contrasts were equal.

7.2. Relevance to models of early spatial vision

Computational models of feature detection in human vision invariably involve a stage in which the image is filtered by linear filters tuned to different scales and orientations (Marr, 1982; Marr & Hildreth, 1980; Moronne & Burr, 1988; Watt, 1988; Watt & Morgan, 1985). These models differ in the way information from different scale filters and from the positive and negative parts of filter outputs are combined to produce a feature description of the image. In Marr's model, image features are indicated by the co-occurrence of zero-crossings in the filter outputs at different scales, but once detected, the feature is labeled for polarity, blur, colour, orientation, contrast, etc. In the MIRAGE model the positive and negative filter outputs are separately combined across scale prior to the stage in which the output is analyzed to provide a symbolic feature description in terms of edges and bars. These models are 'feature-rich' because the luminance scale and contrast-polarity of image features are explicitly represented for higher stages of processing. Other models, such as the local energy model (Moronne & Burr, 1988) locate the position of edges and bars as peaks in the quadratically summed responses of odd- and even-symmetric filters. Although the local energy model allows for energy peaks to be interrogated to determine their phase origin, the model is presumably designed to deliver to higher stages of vision a 'phaseless' energy map. In keeping with this approach, a number of neurophysiological studies have found neurons that are 'form-cue invariant,' that is selective for attributes such

as contour orientation or direction of motion but agnostic as to whether the contours are defined by luminance, contrast or texture (Albright, 1992; Chaudhuri & Albright, 1997; Leventhal, Wang, Schmolesky, & Zhou, 1998). On the other hand, neurophysiological studies of macaque anterior inferotemporal (IT) cortex have shown that individual IT cells involved in encoding shape preserve information about luminance contrast polarity (Ito et al., 1994) and are therefore not form-cue invariant. Our finding that the SFAE is selective for luminance contrast polarity is consistent with the latter neurophysiology and with feature-rich models of early vision.

7.3. Relationship to neurophysiology

Do our results tell us anything about the neural locus for contour shape processing? Although we have not measured the spatial extent over which the SFAE extends the fact that we were able to induce opposite SFAEs from pairs of adaptors only 4 deg (Fig. 1a) apart suggests that the SFAE must be to some extent retinotopically specific. This makes it likely that the SFAE is mediated by a visual area(s) that is retinotopically organized, and a possible candidate is area V4. Neurophysiological studies have shown that neurons in area V4 are involved in coding angles and curves (Pasupathy & Connor, 1999, 2001, 2002) as well as high-level shape information (Desimone & Schein, 1987; Gallant et al., 1993, 1996; Kobatake & Tanaka, 1994). V4 cells have relatively small receptive fields and exhibit selectivity for, among other dimensions, luminance spatial frequency (Desimone, Schein, Moran, & Ungerleider, 1985; Desimone & Schein, 1987). However, we are not aware of any neurophysiological studies that have examined whether V4 cells are selective for luminance contrast polarity.

Acknowledgment

This research was supported by a Natural Sciences and Engineering Research Council of Canada (NSERC) Grant # OGP01217130 given to F.K.

Appendix A. Contour construction

The standard method for constructing sinusoidally shaped contours is to shift the luminance profile 'up and down' along the contour's axis (e.g. Anderson et al., 2005; Habak et al., 2004; Hess et al., 1999; Loffler et al., 2003; Wilkinson et al., 1998). We term this the 'shear' method. If one defines the width of a contour as the length of the line of pixels running perpendicular to the tangent of the contour, then for low amplitudes and spatial frequencies the shear method produces contours of near-constant width. However for moderate to high amplitudes/spatial-frequencies the width of the contour varies significantly along its length, being largest at the peaks and troughs and smallest at the d.c. Moreover, the designated

luminance profile is only ever perpendicular to the tangent of the contour at the peak and trough. These artifacts can be seen in the upper contour in Fig. 6a. With the shear method the ratio of the width of the contour at the d.c. to that at the peak/trough is $\cos(\tan^{-1}(2\pi Af))$, where A is shape amplitude and f shape frequency, both in units of distance. For the contour in Fig. 6a this ratio is 0.52, i.e. the width of the contour at the peak/trough is nearly double that at the d.c. For many purposes this may not be a problem, but given that we wanted to study the width tuning of the SFAE, we felt it important to use contours with constant width and with luminance profiles that were always perpendicular to the tangent.

There are many ways to produce sinusoidal contours of constant width. One way is to use the shear method but vary the length of the line of pixels as it is shifted up and down to compensate for the effects of the shear. However, this does not solve the problem of the orientation of the luminance profile. Another potential solution is to draw a single-grey-level hard-edged contour of fixed width and then convolve this with a kernel such as an isotropic Gaussian, or Gabor filter. However, the contour's luminance profile will not be uniform along its length, having a higher contrast at its peaks and troughs than at its d.c.

Here, we describe a method for producing sinusoidal contours of constant width and perpendicular-to-tangent luminance profiles (Fig. 6b). Consider a line of pixels running along the centre of the sinusoidal-shaped contour. This is shown in Fig. 6c as the dashed line and is given by the equation:

$$y(x) = A \sin(2\pi fx + \rho), \quad (\text{AI.1})$$

where y is the vertical relative to mean pixel position, A shape amplitude in pixels, f shape-frequency in cycles per pixel and ρ shape-phase in radians. We start by drawing a new line of pixels at a distance $w/2$ perpendicular to the dashed line. This is the continuous line in Fig. 6c and it is defined by the following equation:

$$y(x - \Delta x) = A \sin(2\pi fx + \rho) - \Delta y \quad (\text{AI.2})$$

$$\begin{aligned} \text{where } \Delta x &= w/2 \cdot \sin\theta, \\ \Delta y &= w/2 \cdot \cos\theta \\ &\text{and} \end{aligned}$$

$$\theta = \tan^{-1}[A2\pi f(2\pi fx + \rho)]. \quad (\text{AI.3})$$

Next, we draw a second line (not shown) on the other side of the dashed line by setting $w/2$ to negative. To 'fill in' the rest of the contour we repeat the above procedure, decreasing $w/2$ each time by a small amount until it reaches zero. When drawing each line it is important to increment x by a sub-pixel amount, otherwise gaps appear in the resulting profile. The size of the increment necessary to avoid gaps needs to be inversely proportional to the curvature, but we found that an increment of a quarter of a pixel was sufficient for most purposes. At high curvatures the lines double back on themselves at the peaks and troughs of the waveform, but if drawn from the outside inwards, each line overwrites part of the doubled back portion of the previous line, such that when $w/2$ reaches zero the contour is completely 'clean.'

The pixel intensities allocated to each line are in accordance with the desired luminance profile (see Section 2).

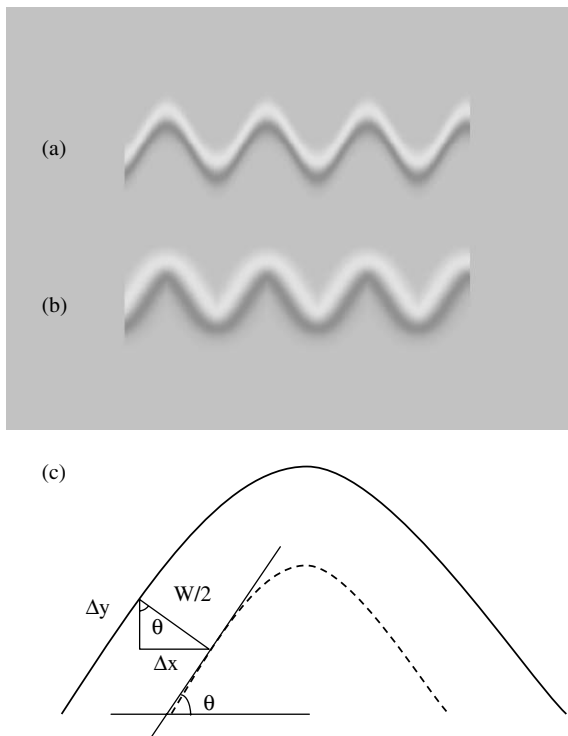


Fig. 6. Example contours drawn using (a) the conventional 'shear' and (b) our 'constant-width' method (see Appendix A for details).

References

- Albright, T. D. (1992). Form-cue invariant motion processing in primate visual cortex. *Science*, 255, 1141–1143.
- Anderson, N. D., Habak, C., Wilkinson, F., & Wilson, H. R. (2005). Evaluating curvature aftereffects with radial frequency contours. *Journal of Vision*, 5(7), 209 [Abstract].
- Anderson, N. D., & Wilson, H. R. (2005). The nature of synthetic face adaptation. *Vision Research*, 45, 1815–1828.
- Blake, R., Overton, R., & Lema-Stern, S. (1981). Interocular transfer of visual aftereffects. *Journal of Experimental Psychology: Human Perception and Performance*, 7(2), 367–381.
- Blakemore, C., & Over, R. (1974). Curvature detectors in human vision? *Perception*, 3, 3–7.
- Blakemore, C., & Sutton, P. (1969). Size adaptation: a new aftereffect. *Science*, 166, 245–247.
- Bonds, A. B. (1989). Role of inhibition in the specification of orientation selectivity of cells in the cat striate cortex. *Visual Neuroscience*, 2(1), 41–55.
- Bonds, A. B. (1991). Temporal dynamics of contrast gain in single cells of the cat striate cortex. *Visual Neuroscience*, 6(3), 239–255.
- Burton, G. J., Nagshineh, S., & Ruddock, K. H. (1977). Processing by the human visual system of the light and dark contrast components of the retinal image. *Biological Cybernetics*, 27(4), 189–197.
- Chaudhuri, A., & Albright, T. D. (1997). Neuronal responses to edges defined by luminance vs. temporal texture in macaque area V1. *Visual Neuroscience*, 14(5), 949–962.
- Desimone, R., Schein, S. J., Moran, J., & Ungerleider, L. G. (1985). Contour, color and shape analysis beyond the striate cortex. *Vision Research*, 25(3), 441–452.

- Desimone, R., & Schein, S. J. (1987). Visual properties of neurons in area V4 of the macaque: sensitivity to stimulus form. *Journal of Neurophysiology*, 57(3), 835–868.
- DeValois, K. K. (1977a). Independence of black and white: phase-specific adaptation. *Vision Research*, 17, 209–215.
- DeValois, K. K. (1977b). Spatial frequency adaptation can enhance contrast sensitivity. *Vision Research*, 17(9), 1057–1065.
- DeValois, R. L., & DeValois, K. K. (1988). *Spatial vision*. Oxford: Oxford University Press.
- Durgin, F. H. (1996). Visual aftereffect of texture density contingent on color of frame. *Perception and Psychophysics*, 58(2), 207–223.
- Durgin, F. H. (2001). Texture contrast aftereffects are monocular; texture density aftereffects are binocular. *Vision Research*, 41(20), 2619–2630.
- Durgin, F. H., & Proffitt, D. R. (1996). Visual learning in the perception of texture: simple and contingent aftereffects of texture density. *Spatial Vision*, 9(4), 423–474.
- Durgin, F. H., & Huk, A. C. (1997). Texture density aftereffects in the perception of artificial and natural textures. *Vision Research*, 37(23), 3273–3282.
- Elder, J. H., & Sachs, A. J. (2004). Psychophysical receptive fields of edge detection mechanisms. *Vision Research*, 44(8), 795–813.
- Fiorentini, A., Baumgartner, G., Magnusson, S., Schiller, P. H., & Thomas, J. P. (1990). The perception of brightness and darkness: Relations to neuronal receptive fields. In L. Spillman & J. S. Werner (Eds.), *Visual perception: The neurophysiological foundations*. San Diego, CA: Academic Press.
- Gallant, J. L., Braun, J., & van Essen, D. C. (1993). Selectivity for polar, hyperbolic and Cartesian gratings in macaque visual cortex. *Science*, 259(5091), 1100–1103.
- Gallant, J. L., Connor, C. E., Rakshit, S., Lewis, J. W., & van Essen, D. C. (1996). Neural responses to polar, hyperbolic and Cartesian gratings in area V4 of the macaque monkey. *Journal of Neurophysiology*, 76(4), 2718–2839.
- Greenlee, M. W., & Heitger, F. (1988). The functional role of contrast adaptation. *Vision Research*, 28(7), 791–797.
- Greenlee, M. W., & Thomas, J. P. (1992). Effect of pattern adaptation on spatial frequency discrimination. *Journal of the Optical Society of America A*, 9(6), 857–862.
- Greenlee, M. W., & Thomas, J. P. (1993). Simultaneous discrimination of the spatial frequency and contrast of periodic stimuli. *Journal of the Optical Society of America A*, 10(3), 395–404.
- Gross, C. G. (1992). Representation of visual stimuli in inferior temporal cortex. *Philosophical Transactions of the Royal Society London Series B*, 335(1273), 3–10 [Review].
- Habak, C., Wilkinson, F., Zahker, B., & Wilson, H. R. (2004). Curvature population coding for complex shapes in human vision. *Vision Research*, 44, 2815–2823.
- Hanly, M., & MacKay, D. M. (1979). Polarity-sensitive perceptual adaptation to sawtooth modulation of luminance. *Experimental Brain Research*, 35(1), 37–46.
- Hammett, S. T., Snowden, R. J., & Smith, A. T. (1994). Perceived contrast as a function of adaptation duration. *Vision Research*, 34(1), 31–40.
- Harris, J. P., & Calvert, J. E. (1989). Contrast, spatial frequency and test duration effects on the tilt aftereffect: implications for underlying mechanisms. *Vision Research*, 29(1), 129–135.
- Hayes, A., Kingdom, F. A. A., & Prins, N. (2002). The detection of smooth curves in jagged contours. *Perception*, 31(supplement), 153 [Abstract].
- He, Z. J., & Ooi, T. L. (1998). Illusory-contour formation affected by luminance contrast polarity. *Perception*, 27(3), 313–335.
- Heeger, D. J. (1992). Normalization of cell responses in cat striate cortex. *Visual Neuroscience*, 9(2), 181–197.
- Held, R., Shattuck-Hufnagel, S., & Moskowitz, A. (1982). Color-contingent tilt aftereffect: spatial frequency specificity. *Vision Research*, 22(7), 811–817.
- Hess, R. F., Wang, Y. Z., & Dakin, S. C. (1999). Are judgments of circularity local or global? *Vision Research*, 39(26), 4354–4360.
- Hesse, G. S., & Georgeson, M. A. (2005). Edges and bars: where do people see features in 1D images? *Vision Research*, 45(4), 507–525.
- Huang, P.-C., Kingdom, F. A. A., & Hess, R. F. (2006). Two phase mechanisms, $\pm\cosine$, in human vision. *Vision Research*, 46(13), 2069–2081.
- Ito, M., Fujita, I., Tamura, H., & Tanaka, K. (1994). Processing of contrast polarity of visual images in inferotemporal cortex of the macaque monkey. *Cerebral cortex*, 4(5), 499–508.
- Keeble, D. R. T., & Hess, R. F. (1999). Discriminating local continuity in curved figures. *Vision Research*, 39, 3287–3299.
- Kingdom, F. A. A., & Gheorghiu, E. (2006). On the mechanisms for contour-shape after effects. *Journal of Vision*, 6(6), 339a.
- Kingdom, F. A. A., & Prins, N. (2005a). Different mechanisms encode the shapes of contours and contour-textures. *Journal of Vision*, 5(8), 463 [Abstract].
- Kingdom, F. A. A., & Prins, N. (2005b). Separate after-effects for the shapes of contours and textures made from contours. *Perception*, 34(supplement), 92 [Abstract].
- Kobatake, E., & Tanaka, K. (1994). Neuronal selectivities to complex object features in the ventral visual pathway of the macaque cerebral cortex. *Journal of Neurophysiology*, 71(3), 856–867.
- Kramer, D., & Fahle, M. (1996). A simple mechanism for detecting low curvatures. *Vision Research*, 36(10), 1411–1419.
- Koenderink, J. J., & Richards, W. (1988). Two-dimensional curvature operators. *Journal of the Optical Society of America A*, 5, 1136–1141.
- Leventhal, A. G., Wang, Y., Schmolesky, M. T., & Zhou, Y. (1998). Neural correlates of boundary perception. *Visual Neuroscience*, 15(6), 1107–1118.
- Levi, D. M., & Klein, S. A. (2000). Seeing circles: what limits shape perception? *Vision Research*, 40(17), 2329–2339.
- Loffler, G., Wilson, H. R., & Wilkinson, F. (2003). Local and global contributions to shape discrimination. *Vision Research*, 43, 519–530.
- Magnussen, S., & Kurtenbach, W. (1979). A test for contrast-polarity selectivity in the tilt aftereffect. *Perception*, 8(5), 523–528.
- Marr, D. (1982). *Vision: A computational investigation into the human representation and processing of visual information*. San Francisco: W.H. Freeman.
- Marr, D., & Hildreth, E. (1980). Theory of edge detection. *Proceedings of the Royal Society of London B*, 207, 187–217.
- Moronne, M. C., & Burr, D. C. (1988). Feature detection in human vision: a phase-dependent energy model. *Proceedings of the Royal Society of London B*, 235, 221–245.
- Pantle, A., & Sekuler, R. (1968). Size-detecting mechanisms in human vision. *Science*, 6, 162(858), 1146–1148.
- Pasupathy, A., & Connor, C. E. (1999). Responses to contour features in macaque area V4. *Journal of Neurophysiology*, 82(5), 2490–2502.
- Pasupathy, A., & Connor, C. E. (2001). Shape representation in area V4: position-specific tuning for boundary conformation. *Journal of Neurophysiology*, 86(5), 2505–2519.
- Pasupathy, A., & Connor, C. E. (2002). Population coding of shape in area V4. *Nature Neuroscience*, 5(12), 1332–1338.
- Regan, D., & Hamstra, S. J. (1992). Shape discrimination and the judgment of perfect symmetry: dissociation of shape from size. *Vision Research*, 32(10), 1845–1864.
- Rolls, E. T., & Baylis, G. C. (1986). Size and contrast have only small effects on the responses to faces of neurons in the cortex of the superior temporal sulcus of the monkey. *Experimental Brain Research*, 65(1), 38–48.
- Scalar, G., Ohzawa, I., & Freeman, R. D. (1982). Contrast gain control in the cat visual cortex. *Nature*, 298(5871), 266–268.
- Scalar, G., Ohzawa, I., & Freeman, R. D. (1985). Contrast gain control in the cat's visual system. *Journal of Neurophysiology*, 54(3), 651–657.
- Schiller, P. H. (1982). Central connections of the retinal ON and OFF pathways. *Nature*, 297(5867), 580–583.
- Schiller, P. H. (1984). The connections of the retinal on and off pathways to the lateral geniculate nucleus of the monkey. *Vision Research*, 24(9), 923–932.

- Schiller, P. H., Sandell, J. H., & Maunsell, J. H. (1986). Functions of the ON and OFF channels of the visual system. *Nature*, 322(6082), 824–825.
- Snowden, R. J. (1994). Adaptability of the visual system is inversely related to its sensitivity. *Journal of the Optical Society of America A, Optics and Image Science*, 11(1), 25–32.
- Stromeyer, C. F., 3rd, & Riggs, L. A. (1974). Curvature detectors in human vision? *Science* 184(142), 1199–1201.
- Suzuki, S. (2001). Attention-dependent brief adaptation to contour orientation: a high-level aftereffect for convexity? *Vision Research*, 41, 3883–3902.
- Suzuki, S. (2003). Attentional selection of overlapped shapes: a study using brief shape aftereffects. *Vision Research*, 43, 549–561.
- Suzuki, S., & Cavanagh, P. (1998). A shape-contrast effect for briefly presented stimuli. *Journal of Experimental Psychology: Human Perception and Performance*, 24(5), 1315–1341.
- Tanaka, K. (1996). Inferotemporal cortex and object vision. *Annu. Rev. Neurosci.*, 19, 109–139.
- Tyler, C. W. (1973). Periodic vernier acuity. *Journal of Physiology*, 228(3), 637–647.
- Yamashita, J. A., Hardy, J. L., De Valois, K. K., & Webster, M. A. (2005). Stimulus selectivity of figural aftereffects for faces. *Journal of Experimental Psychology: Human Perception and Performance*, 31(3), 420–437.
- Watt, R. J. (1988). *Visual processing*. Hove and London: L Erlbaum Associates.
- Watt, R. J., & Andrews, D. P. (1982). Contour curvature analysis: hyperacuity in the discrimination of detailed shape. *Vision Research*, 22(4), 449–460.
- Watt, R. J., & Morgan, M. J. (1985). Spatial filters and the localization of luminance changes in human vision. *Vision Research*, 24(10), 1387–1397.
- Wilkinson, F., Wilson, H. R., & Habak, C. (1998). Detection and recognition of radial-frequency patterns. *Vision Research*, 38, 3555–3568.
- Wilson, H. R. (1986). Responses of spatial mechanisms can explain hyperacuity. *Vision Research*, 26(3), 453–469.
- Wilson, H. R. (1991). Pattern discrimination, visual filters and spatial sampling irregularity. In Movshon J. A. & Landy M. S: *Computational models of visual processing*.
- Wilson, H. R., & Humanski, R. (1993). Spatial frequency adaptation and contrast gain control. *Vision Research*, 33(8), 1133–1149.
- Wilson, H. R., & Richards, W. A. (1989). Mechanisms of contour curvature discrimination. *Journal of the Optical Society of America A*, 6, 106–115.
- Wilson, H. R., & Richards, W. A. (1992). Curvature and separation discrimination at texture boundaries. *Journal of the Optical Society of America A*, 9(10), 1653–1662.